Paleoceanography and Paleoclimatology

RESEARCH ARTICLE
10.1029/2021PA004319

Key Points:

- Coral boron systematics bear considerable intercolony differences
- Fossil corals aged within the past 1 ka have higher pH_{cf} but equivalent DIC_{cf} levels compared to the modern corals
- Significant post-industrial pH_{sw} decline occurred in the northern South China Sea

Supporting Information:

Supporting Information may be found in the online version of this article.

Correspondence to:

X. Chen,
chenxf@gig.ac.cn

Citation:

Chen, X., Deng, W., Kang, H., Zeng, T., Zhang, L., Zhao, J.-x., & Wei, G. (2021). A replication study on coral $\delta^{11}B$ and B/Ca and their variation in modern and fossil *Porites*: Implications for coral calcifying fluid chemistry and seawater pH changes over the last millennium. *Paleoceanography and Paleoclimatology*, *36*, e2021PA004319. https://doi.org/10.1029/2021PA004319

Received 3 JUN 2021
Accepted 26 SEP 2021

A Replication Study on Coral $\delta^{11}B$ and B/Ca and Their Variation in Modern and Fossil *Porites*: Implications for Coral Calcifying Fluid Chemistry and Seawater pH Changes Over the Last Millennium

Xuefei Chen[1,2,3], Wenfeng Deng[1,2,3], Huiling Kang[1,2,3], Ti Zeng[2,3,4], Le Zhang[1,2], Jian-xin Zhao[5], and Gangjian Wei[1,2,3]

[1]State Key Laboratory of Isotope Geochemistry, Guangzhou Institute of Geochemistry, Chinese Academy of Sciences, Guangzhou, China, [2]CAS Center for Excellence in Deep Earth Science, Guangzhou, China, [3]Southern Marine Science and Engineering Guangdong Laboratory (Guangzhou), Guangzhou, China, [4]Key Laboratory of Marginal Sea Geology, Guangzhou Institute of Geochemistry, Chinese Academy of Science, Guangzhou, China, [5]School of Earth and Environmental Sciences, Radiogenic Isotope Facility, The University of Queensland, Brisbane, QLD, Australia

Abstract Boron systematics offer a unique opportunity to reveal coral calcifying fluid (CF) chemistry and seawater pH (pH_{sw}). Here, we assess the intercolony differences of skeletal $\delta^{11}B$ and B/Ca, and examine their variation in modern and fossil *Porites* spp. collected from the east Hainan Island in the northern South China Sea (SCS), to explore changes in coral CF chemistry and pH_{sw} over the last millennium. This enables us to assess whether ocean acidification (OA) has disturbed the ability of corals to control their CF chemistry, and whether splicing coral $\delta^{11}B$-pH records can trace long-term pH_{sw} variability. We demonstrate that coral boron systematics bear remarkable intercolony differences, with mean offset as high as 1.05‰ for $\delta^{11}B$ and 183.1 μmol/mol for B/Ca. With this in mind, we show that fossil corals exhibit no significant difference in their CF carbonate chemistry, but all have systematically higher CF pH (pH_{cf}, by an average of 0.12 units) and almost equivalent CF dissolved inorganic carbon (DIC_{cf}) concentration, compared to modern corals. This suggests greater OA impacts on coral pH_{cf} but less noticeable effects on DIC_{cf}. In addition, the ~0.12 decline in pH_{cf} translates to about 0.24 reduction in pH_{sw}, similar to another coral-based estimate (~0.24) from south Hainan Island, corroborating significant OA in the northern SCS since the industrial era. Nevertheless, we find that pH_{sw} in the east Hainan Island has staged a recovery from 1980 to 2010, slowing down the OA pace, highlighting important roles of other local forcing on pH_{sw} regulation.

1. Introduction

Reef-building corals are among the most sensitive marine organisms to environmental changes, and as such are of particular concern for their future fate in a changing ocean (Hoegh-Guldberg et al., 2007). Nevertheless, thanks to this sensibility, it also makes coral a natural and accurate recorder of climate change, providing access to the pre-instrumental variability (Gagan et al., 2000).

Boron isotopic composition ($\delta^{11}B$) in coral aragonitic skeleton is an important proxy for seawater pH (pH_{sw}; Hemming & Hanson, 1992; Hemming et al., 1998), as skeletal $\delta^{11}B$ has a strong pH dependency. However, since corals precipitate their calcium carbonate skeleton from an internal calcifying fluid (CF) that is semi-closed to seawater, $\delta^{11}B$-derived pH is primarily interpreted as the pH of CF (pH_{cf}), and then translated into pH_{sw}, provided that there is a constant species-specific pH_{cf} -pH_{sw} relationship. In addition, B/Ca in aragonite is controlled by CO_3^{2-} concentration in the precipitation fluid (Holcomb et al., 2016). Thus, coral boron systematics enable us to fully resolve the carbonate chemistry of coral CF, which has shown that corals favor a distinct CF with both elevated pH_{cf} and DIC_{cf} compared to seawater (Chalk et al., 2021; Chen et al., 2019; D'Olivo et al., 2017, 2019; McCulloch et al., 2017; Ross et al., 2017).

Over the past two decades, a large number of coral-based $\delta^{11}B$-pH records from worldwide reefs have been reported, with most registering an evident signal of ocean acidification (Chen et al., 2019; D'Olivo et al., 2019, 2015; Goodkin et al., 2015; Kubota et al., 2017; Liu et al., 2014; Pelejero et al., 2005; Shinjo et al., 2013; Wei et al., 2009, 2015; Wu et al., 2018). Superimposed on this long-term OA-related downward

trend, is prominent inter-annual to inter-decadal variation that shows linkages with climate variabilities, such as Pacific Decadal Oscillation (Pelejero et al., 2005; Wei et al., 2009), East Asian Monsoon (Liu et al., 2014; Wei et al., 2015), North Atlantic Oscillation (Goodkin et al., 2015), and El Niño-Southern Oscillation (Wu et al., 2018), underlining the important controls of ocean-atmosphere system on pH_{sw}. Importantly, these records also demonstrate that OA has shifted the pH_{cf} of scleractinian corals toward lower values (Chen et al., 2019; D'Olivo et al., 2019; Goodkin et al., 2015; Kubota et al., 2017; Liu et al., 2014; Wei et al., 2009; Wu et al., 2018), which then reduces the concentration of CO_3^{2-} in the CF ($[CO_3^{2-}]_{cf}$) (Chen et al., 2019; D'Olivo et al., 2019), a critical parameter controlling calcification. Nevertheless, it appears that DIC_{cf} remains constant over the past decades, showing no clear or a slightly increase in response to climate change (Chen et al., 2019; D'Olivo et al., 2019), indicating that the coral's capacity to concentrate carbon for calcification is less disturbed.

Typically, these coral-based boron systematics reconstructions are mainly derived from living colonies, with growth length no longer than 400 years (e.g., Chen et al., 2019; D'Olivo et al., 2019, 2015; Fowell et al., 2018; Goodkin et al., 2015; Pelejero et al., 2005; Wei et al., 2009; Wu et al., 2018). Only a few studies have applied δ^{11}B-pH to fossil corals to obtain extended records (Douville et al., 2010; Liu et al., 2009; Raddatz et al., 2016). Accordingly, we know less about the CF carbonate chemistry of ancient corals and whether they have been changed significantly by modern environmental stresses. In addition, this also limits our knowledge of the pre-industrial pH_{sw} changes, in particular over the time frame with natural climate variability that might be expected for the present century in the absence of anthropogenic influence, for example, the past 1–2 millennia. However, while coral paleoclimate studies usually turn to fossil corals to extend reconstruction (e.g., Cobb et al., 2003), splicing boron records is potentially risky due to the possible intercolony differences in skeletal δ^{11}B and B/Ca. This is because skeletal boron systematics are mainly controlled by CF carbonate chemistry, which, although supplied by external seawater, is primarily controlled by the organism (Tambutté et al., 2011).

In this study, we attempt to assess the intercolony differences of boron systematics (δ^{11}B and B/Ca) for *Porites* spp., by comparing the absolute difference and mean difference between the coeval determinations. To achieve this, we select five sets of living *Porites* spp. collected across six reef sites, from both previously reported and new measurements (Figure S1 in Supporting Information S1), to illustrate a general level of intercolony differences for coral boron systematics. Then, we further examine the δ^{11}B and B/Ca of four fossil *Porites* spp. aged within the past millennium, collected from the east coast of Hainan Island in the northern SCS, and compare them with the modern corals from the same reef. By doing so, we explore the changes in coral internal carbonate chemistry, and attempt to reconstruct the pH_{sw} variation over the past millennium with intercolony differences considered.

2. Materials and Methods

2.1. Sample Collection

Four fossil coral cores (11QG1, 11QG3, 11LW2, and 13OC4) and three living coral cores (11LW4, 15WC23, and 15WC26) were collected from *Porites* spp. colonies at water depths of 4–6 m on the reef flat of fringing reefs, off the east coast of Hainan Island in the northern SCS (Figure 1). With the exception of 15WC23 and 15WC26, the other corals have been previously used to study the decadal-to centennial-scale variability in the northern SCS, with Sr/Ca, δ^{13}C, and δ^{18}O being reported in Deng, Chen, et al. (2017), Deng, Liu, et al. (2017), and Deng et al. (2013) and the δ^{11}B results of 11LW4 being reported in Wei et al. (2015).

Drill cores 10AR2 were collected in April 2010 from a living *Porites* sp. coral colony at a water depth of ~4 m on Arlington Reef in the mid-shelf GBR (Figure S1 in Supporting Information S1). This coral is in proximity to a previously reported coral AREO 4 for δ^{11}B-pH study (Wei et al., 2009) and was thus adopted for the δ^{11}B individual differences evaluation.

Coral cores were first sectioned into slices with a thickness of 1 cm and width of 5–7 cm. Then, the slabs were X-ray photographed to reveal the density bands (Figure S2 in Supporting Information S1), which served as a reference for coral chronology and subsampling. Next, coral slabs were immersed in 10% H_2O_2 for 24 hr to remove organic matter, followed by thorough ultrasonic cleaning in deionized water for 3 × 10 min to eliminate surface contaminants, and then were dried at 50°C. For fossil corals, a small subsample (5 cm^3)

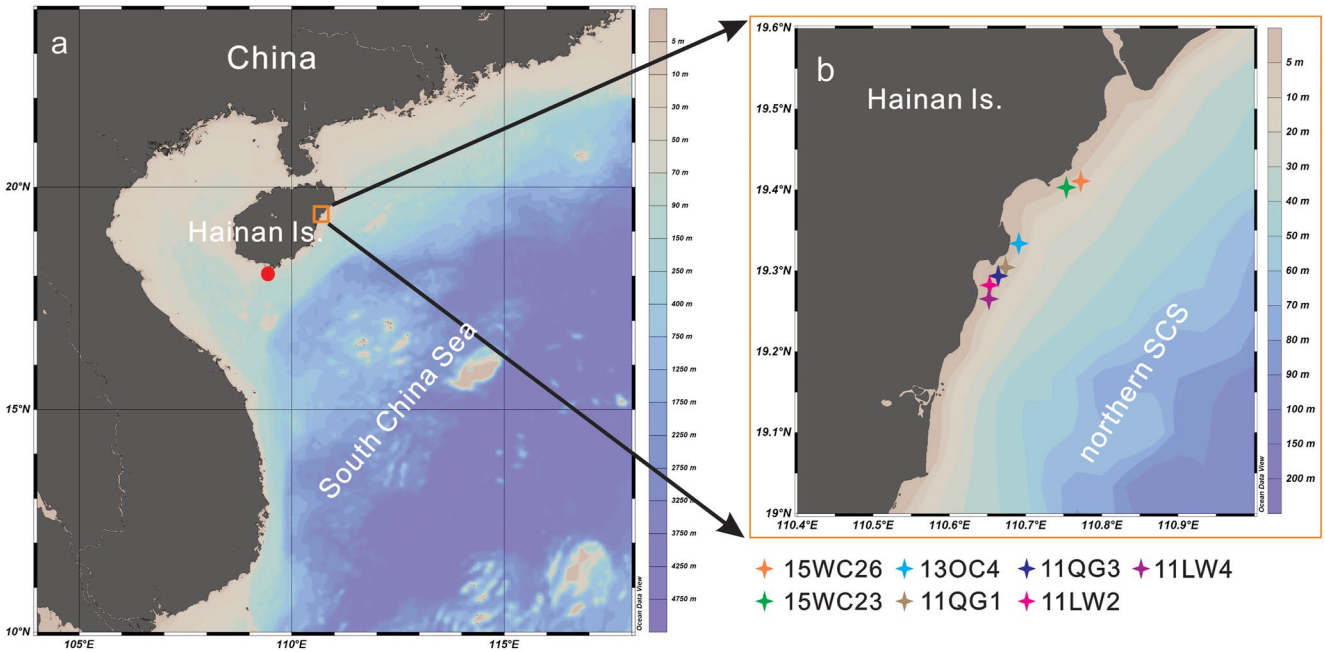

Figure 1. (a) Map of the South China sea and study area; (b) Sampling sites of the studied corals shown with stars. Red dot in panel (a) indicates a previously reported coral-$\delta^{11}B$ study from the south coast of Hainan (Liu et al., 2014).

from the upper part of each core was cut using a diamond blade saw and prepared for U-Th dating. For corals 15WC23 and 15WC26, two-year-resolution samples were collected along the main growth axis using a computer-controlled micromill, with each high- and low-density band representing 1 year of coral growth. With respect to the rest of corals, annual samples were collected along the main growth axis. The detailed sampling tracks are illustrated in Figure S2 in Supporting Information S1. For the modern coral 11LW4, its $\delta^{11}B$ determination was reported in Wei et al. (2015). In this study, the powder samples of this coral core were newly collected along the previous sampling tracks as described in Figure 2 of Chen et al. (2015).

To test for potential early diagenesis in fossil corals, 12 subsamples from all the coral cores were systematically cut, with 4 subsamples for each longer core (i.e., 11QG1 and 13OC4) and 2 for each shorter core (i.e., 11QG3 and 11LW2). Each subsample was further divided into two portions for powder X-ray diffraction (XRD) and scanning electron microscopy (SEM) analyses at the Guangzhou Institute of Geochemistry, Chinese Academy of Science. XRD results show that the coral skeleton was 100% aragonite (Figure S3 in Supporting Information S1), and SEM imaging reveals that there was no secondary aragonite present in the coral skeleton (Figure S4 in Supporting Information S1).

2.2. Chronology

The ages of the fossil corals were determined by U-Th measurements, using the multi-collector inductively coupled plasma mass spectrometers (MC-ICP-MS) at the Radiogenic Isotope Laboratory of the University of Queensland and the High-precision Mass Spectrometry and Environment Change Laboratory of the National Taiwan University. Detailed analytical methods and results were reported in our previous studies (Deng, Chen, et al., 2017; Deng, Liu, et al., 2017; results also shown in Table S1 in Supporting Information S1). Coral samples of the age control points for 11QG1, 11QG3, 11LW2, and 13OC4 were dated 756 ± 9.6, 929 ± 24, 371 ± 18, and 254 ± 4 year B.P., respectively (Table S1 in Supporting Information S1). The chronology of fossil corals was then established by counting the annual bands backward and forwards from the U-Th dated calendar year of the age control point. When the dated ages were transformed into Common Era years, their growing intervals covered approximately 1129–1255 CE, 1063–1087 CE, 1628–1657 CE, and 1702–1772 CE, respectively, which fell into two main climate epochs over the past 1 ka, that is, the Medieval Climate Anomaly (MCA, 900–1300 CE) and the Little Ice Age (LIA, 1550–1850 CE).

2.3. Boron Systematics

Measurements of boron isotopes and B/Ca ratios were carried out at the State Key Laboratory of Isotope Geochemistry, Guangzhou Institute of Geochemistry, Chinese Academy of Science. For cores 11LW4, 11QG1, 11QG3, 11LW2, and 13OC4, their $\delta^{11}B$ and B/Ca were processed separately. Approximately 5 mg annual sample powders were dissolved in 0.51 M HNO_3, with subaliquots diluted in 2% HNO_3 to measure B/Ca ratios using an iCAP Q ICP-MS (Thermo Fisher Scientific). Coral standard JCp-1 was measured along with the samples to monitor the precision of the analysis, yielding an averaged B/Ca value of 466.8 ± 14.3 μmol/mol (SD, $n = 10$), which was consistent with the reported 459.6 ± 22.7 μmol/mol in Hathorne et al. (2013). Boron purification for the fossil coral samples and 10AR2 followed the procedures described in Wei et al. (2009, 2015). Approximately 20 mg of annual sample was weighted, dissolved in 0.2 mL of 3 M HNO_3 and diluted to 1 mL with 0.1 M HNO_3. Then, the solution was first loaded onto the column containing Bio-Rad AG50W-X8 cation resin to remove the Ca matrix, followed by a second column containing Amberlite IRA 743 resin to concentrate and purify B. The $\delta^{11}B$ measurements were carried out on a Neptune Plus multi-collector inductively coupled plasma mass spectrometer (MC-ICP-MS, Thermo Fisher Scientific), following the measurement strategy described in Wei et al. (2015). Multiple measurements of JCp-1 yielded an average $\delta^{11}B$ value of 24.18 ± 0.40‰ (2SD, $n = 10$), which was consistent with the previously reported values (e.g., McCulloch et al., 2014).

For coral cores 15WC23 and 15WC26, we adopted a more efficient method described in McCulloch et al. (2014), with $\delta^{11}B$ and B/Ca being measured from the same weighted samples. Briefly, about 10 mg of sample powder was dissolved in 0.5 mL of 0.51 M HNO_3, with a small aliquot of 95 μL diluted in 7.5 mL 2% HNO_3 to a final concentration of ~100 ppm Ca for B/Ca measurements via ICP-MS. The rest of the sample solution (~400 μL) was loaded onto the preconditioned column, which contained 0.6 mL AG50W-X8 resin above 1.0 mL AG1-X8 resin to remove the cation (e.g., Ca, Mg, and Sr) and anion (e.g., SO_4^{2-}) matrices, respectively. The column was then eluted with 6 × 0.5 mL 0.075 M HNO_3, yielding a ~100 ppb B solution ready for $\delta^{11}B$ analysis via MC-ICP-MS. The coral standard JCp-1 was chemically treated with the same procedures as the samples and was measured repeatedly with the samples, yielding an average B/Ca values of 472.9 ± 12.5 μmol/mol (SD, $n = 4$) and $\delta^{11}B$ value of 24.42 ± 0.36‰ (2σ, $n = 4$), within the analytical error of previously reported values (Hathorne et al., 2013; McCulloch et al., 2014).

2.4. Estimates for Coral Calcifying Fluid Carbonate Chemistry and Seawater pH

The boron isotopic composition of the coral skeleton ($\delta^{11}B_{coral}$) is believed to be mainly inherited from the $\delta^{11}B$ signature of borate ions ($\delta^{11}B_{(B(OH)4-)}$) in coral extracellular CF, of which the fractionation is pH-dependent. Thus, coral pH_{cf} can be estimated from the following equation (Zeebe & Wolf-Gladrow, 2001):

$$pH_{cf} = pK_B - \log\left[\frac{\delta^{11}B_{sw} - \delta^{11}B_{coral}}{\alpha_{B3-B4} \times \delta^{11}B_{coral} - \delta^{11}B_{sw} + 1000\left(\alpha_{B3-B4}\right) - 1}\right] \quad (1)$$

where $\delta^{11}B_{sw}$ is the B isotope composition of seawater ($\delta^{11}B_{sw}$ = 39.61‰; Foster et al., 2010) and the B isotope fractionation factor ($\alpha_{B3\text{-}B4}$) is 1.0272, as estimated by Klochko et al. (2009). The B dissociation constant (pK_B) is well defined by temperature and salinity, with a value of 8.597 at a temperature of 25°C and salinity of 35 (Dickson, 1990). To calculate pH_{cf}, the temperature of coral growth periods was estimated from the Sr/Ca-SST relationship (Deng, Chen, et al., 2017). The salinity was set as 34, as indicated in Dong et al. (2017), and assumed to change little over time.

As the incorporation of $B(OH)_4^-$ substitutes for CO_3^{2-} in the aragonite lattice during $CaCO_3$ precipitation, with the partition coefficient K_D dependent on the solution pH, where $K_D = 2.965\exp(-0.0202[H^+]_T)$ (McCulloch et al., 2017), skeletal B/Ca ratios are used to estimate the concentration of carbonate ions within the CF ($[CO_3^{2-}]_{cf}$). Combined with pH_{cf} derived from $\delta^{11}B_{coral}$ and assuming that $[B]_{cf}$ is equal to the total boron concentration in seawater, $[CO_3^{2-}]_{cf}$ can be calculated with the following equation:

$$\left[CO_3^{2-}\right]_{cf} = K_D \times \frac{\left[B(OH)_4^-\right]_{cf}}{\left(B/Ca\right)_{CaCO_3}} \quad (2)$$

with knowledge of both pH_{cf} and $[CO_3^{2-}]_{cf}$, the DIC_{cf} can then be calculated.

Since seawater provides the primary supply for the chemical composition of coral internal CF, the underlying connection between pH_{sw} and pH_{cf} can be used to estimate pH_{sw} changes from pH_{cf}. The empirical relationship between pH_{sw} and pH_{cf} is obtained from coral culture experiments; thus, pH_{sw} can be estimated by the following equation (Hönisch et al., 2004; McCulloch et al., 2012):

$$pH_{cf} = 0.46 \times pH_{sw} + 4.72 \; P.cylindrica \quad (3)$$

by which we found that the reconstructed pH_{sw} (average of 8.05 ± 0.05) via the three modern corals showed the best agreement with the in situ pH_{sw} measurements (an average of 8.04 ± 0.03 for the measurements in 2014–2015, total scale) in Dong et al. (2017), compared to the pH_{sw} value (average of 7.88 ± 0.05) estimated from the equation specific for massive *Porites* spp. (Krief et al., 2010). While applying the pH_{cf}-pH_{sw} calibration of branching *P.cylindrica* on massive *Porites* spp. seems risky, previous study has demonstrated that this relationship can produce decent results for a *Porites australiensis* (D'Olivo et al., 2019).

2.5. Evaluation of $\delta^{11}B$ and B/Ca Intercolony Variability for *Porites* spp. Coral

The $\delta^{11}B$ determinations of five sets of *Porites* spp. corals (Figure S1 in Supporting Information S1) are adopted to assess the coral intercolony differences, including:

1. Three corals from the east coast of Hainan Island (northern SCS; two-year resolution)
2. Two corals from the Havannah Island and one coral from the nearby Pandora Reef (Great Barrier Reef, GBR; D'Olivo et al., 2015; annual resolution)
3. Two corals from the Arlington Reef (GBR; coral AREO 4 from Wei et al., 2009; and coral 10AR2 from this study; annual resolution)
4. Two corals from the Davies Reef (GBR; McCulloch et al., 2017; monthly resolution)
5. Two corals from the Ningaloo Reef (Western Australia; McCulloch et al., 2017; monthly resolution)

With respect to B/Ca, only three sets of *Porites* spp. corals, that is, (1, 4, 5), are available to assess intercolony differences.

The absolute value of the difference between the coeval $\delta^{11}B$ (or B/Ca) time series is calculated by subtracting the $\delta^{11}B$ (or B/Ca) values of the identical year or month. The average of the absolute difference (avg_{abs}) can be used to assess coral intercolony differences. In addition, the mean difference between the coeval time series is also calculated by subtracting the arithmetic mean average of the two records, which represents the general bias induced by intercolony differences.

3. Results

3.1. Replication Tests of Coral Boron Systematics

3.1.1. $\delta^{11}B$

Boron isotopes of the two adjacent cores 15WC23 and 15WC26 from Hainan Is. varied within the normal $\delta^{11}B$ range (22‰–26‰) for modern *Porites* spp. corals (e.g., Chen et al., 2019; D'Olivo et al., 2019, 2015; Pelejero et al., 2005; Wei et al., 2009, 2015). The two time series exhibited comparable long-term mean values of 24.10‰ and 24.31‰, respectively, but divergent patterns resulted in no correlation between them (Figure 2a). The avg_{abs} between the two time series is about 0.72‰, comparable to the 2σ of the magnitude of analytical precision (0.36‰, 2σ, or magnitude of 0.72‰; Table 1). However, compared with our previously reported coral core 11LW4, which was also collected from the east coast of Hainan Island but ~10 km away from them (Wei et al., 2015), considerable differences ($p < 0.05$; two-sample t tests; Table S2 in Supporting Information S1) were found for the coeval $\delta^{11}B$ determinations (Figure 2a, Table 1), with a large avg_{abs} of 1.19‰ and a moderate mean offset of 0.76‰ between 11LW4 and 15WC26, and an equivalent level avg_{abs} of 1.12‰ and a mean offset of 0.97‰ between 11LW4 and 15WC23.

The $\delta^{11}B$ results of coral 10AR2 from the mid-shelf Arlington Reef in the GBR fluctuated from 22.81 to 24.90‰, also falling within the normal $\delta^{11}B$ variation range, and showed a moderate offset (0.53‰, Table 1, Figure 2b) with the coeval $\delta^{11}B$ determinations of another adjacent colony AREO 4 (reported in Wei et al., 2009). However, patterns of the two time series were divergent, leading to considerable absolute differences with values as large as 2.72‰ ($p < 0.05$; two-sample t tests; Table S2 in Supporting Information S1).

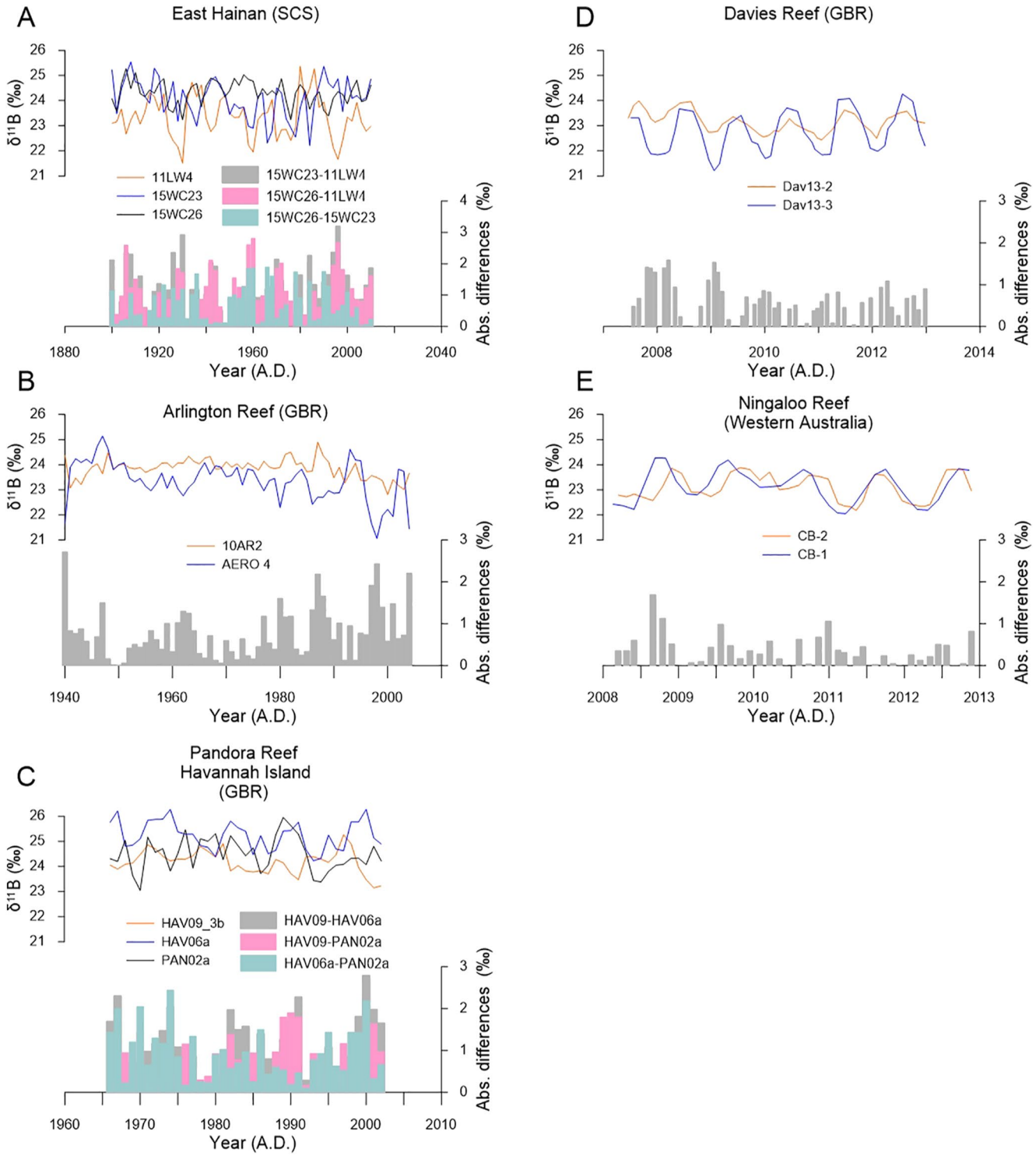

Figure 2. Assessment of $\delta^{11}B$ individual differences for *Porites* spp. corals. Comparisons between the coeval $\delta^{11}B$ determinations of corals from: (a) East Hainan Island (northern SCS, 11LW4 of Wei et al., 2015, 15WC23 and 15WC26 of this study); (b) Arlington Reef (mid-shelf GBR, AREO 4 of Wei et al., 2009 and 10AR2 of this study); (c) Pandora Reef and Havannah Island (inner-shelf GBR, D'Olivo et al., 2015); (d) Davies Reef (mid-shelf GBR, McCulloch et al., 2017); and (e) Ningaloo Reef (Western Australia, McCulloch et al., 2017), respectively. The absolute value of the difference between colonies is shown below each comparison. Note that $\delta^{11}B$ records in (a–c) are biennially or annually resolved, while in panels (d and e) are monthly-resolved.

Table 1
$\delta^{11}B$ Individual Differences of Porites spp. Corals

Sample resolution	Location	Sample name	$\delta^{11}B$ variation range	Analytical precision (2σ)	Mean value		Mean difference		Average absolute difference	
					$\delta^{11}B$	pH_{cf}	$\delta^{11}B$	pH_{cf}	$\delta^{11}B$ (SD)	pH_{cf} (SD)
Annual or Biennial	Pandora Reef, Havannah Island, Inner-shelf GBR	PAN02a[g]	23.04–25.95	0.35	24.49	8.53	0.31[a]	0.02[a]	0.75 (0.51) [a]	0.05 (0.03) [a]
		HAV09_3b[g]	23.14–25.26		24.18	8.51	1.05[b]	0.06[b]	1.09 (0.73) [b]	0.07 (0.05) [b]
		HAV06a[g]	24.22–26.27		25.23	8.57	0.74[c]	0.04[c]	0.93 (0.61) [c]	0.06 (0.04) [c]
	Arlington Reef, Mid-shelf GBR	AREO 4[h]	21.06–25.14	0.35	23.35	8.45	0.53	0.04	0.78 (0.62)	0.05 (0.04)
		10AR2	22.81–24.90	0.40	23.88	8.49				
	Hainan Island, South China Sea	11LW4	21.51–25.36	0.44	23.34	8.45	0.76[d]	0.05[d]	1.19 (0.76) [d]	0.08 (0.05) [d]
		15WC23	22.21–25.54	0.36	24.10	8.50	0.21[e]	0.02[e]	0.72 (0.58) [e]	0.05 (0.04) [e]
		15WC26	23.23–25.27		24.31	8.52	0.97[f]	0.07[f]	1.12 (0.69) [f]	0.07 (0.05) [f]
Monthly	Davies Reef, Mid-shelf GBR	Dav13-2[i]	22.44–23.99	0.32	23.14	8.44	0.52	0.03	0.69 (0.41)	0.05 (0.03)
		Dav13-3[i]	21.21–24.26		22.62	8.41				
	Ningaloo Reef, Western Australia	CB-1[i]	22.05–24.27		23.11	8.44	0.02	0.00	0.44 (0.37)	0.03 (0.02)
		CB-2[i]	22.18–23.88		23.09	8.44				

[a]Difference was calculated from PAN02a-HAV09_3b. [b]Difference was calculated from HAV06a-PAN02a. [c]Difference was calculated from HAV06a-HAV09_3b. [d]Difference was calculated from 15WC23-11LW4. [e]Difference was calculated from 15WC26-15WC23. [f]Difference was calculated from 15WC26-11LW4. [g]Data from D'Olivo et al. (2015). [h]Data from Wei et al. (2009). [i]Data from McCulloch et al. (2017).

Nevertheless, the avg_{abs} of 0.78‰ was still within the 2σ of the magnitude of analytical precision (0.40‰, 2σ, or magnitude of 0.80‰; Table 1).

Significant differences were also observed from the other sets of corals reported in literature (Figure 2; the results of two-sample *t* tests are summarized in Table S2 in Supporting Information S1). Large avg_{abs} of 1.09‰ (Table 1) was found for corals from the Havannah Island (Figures 2c and 2d), much above the 2σ of the magnitude of analytical precision (0.35‰, 2σ, or magnitude of 0.70‰; D'Olivo et al., 2015). In addition, coral $\delta^{11}B$ records from two nearby reefs (i.e., Havannah Island and Pandora Reef) showed intercolony differences of similar magnitude, with 0.75‰ between HAV06a and PAN02a, and 0.93‰ between HAV09_3b and PAN02a (Table 1); this was still larger than the 2σ of the magnitude of analytical precision (0.70‰; D'Olivo et al., 2015). In contrast, monthly-resolution $\delta^{11}B$ determinations of corals from the Davies and Ningaloo Reef displayed moderate individual differences, with avg_{abs} of 0.69‰ and 0.44‰ (Table 1), respectively, compared to the analytical precision (0.32‰, 2σ; or magnitude of 0.64‰). Despite having significant absolute difference, it appears that the mean offset between coeval $\delta^{11}B$ time series is relatively smaller compared to the avg_{abs}, ranging from 0.02 to 1.05‰ with an average of 0.56‰ (Table 1).

Divergent patterns found in the annually resolved $\delta^{11}B$ determinations for each set of corals result in a lack of correlation between the coeval $\delta^{11}B$ time series. However, monthly-resolution $\delta^{11}B$ variations are always related among corals, which is possibly due to the prominent seasonality, as we can still see differences from the coeval time series; for example, differences are evident in the variation amplitude (Figure 2d) and phase offset between the $\delta^{11}B$ records (Figure 2e).

Converting $\delta^{11}B$ into pH_{cf} suggests a mean difference of as large as ~0.07 units for corals from the same reef, which could translate to ~0.14 units bias for the long-term averaged pH_{sw} estimation when assuming a constant pH_{cf}-pH_{sw} relationship ($pH_{sw} = (pH_{cf} - 4.72)/0.46$; this conversion amplifies the impacts of intercolony differences in pH_{cf}).

3.1.2. B/Ca

Skeletal B/Ca also varied dramatically among colonies (Figure 3; the results of two-sample *t* tests are summarized in Table S3 in Supporting Information S1). 11LW4 has the highest B/Ca values with an average of 602.9 μmol/mol, showing large avg_{abs} of 183.7 μmol/mol and 135.3 μmol/mol in comparison to 15WC23

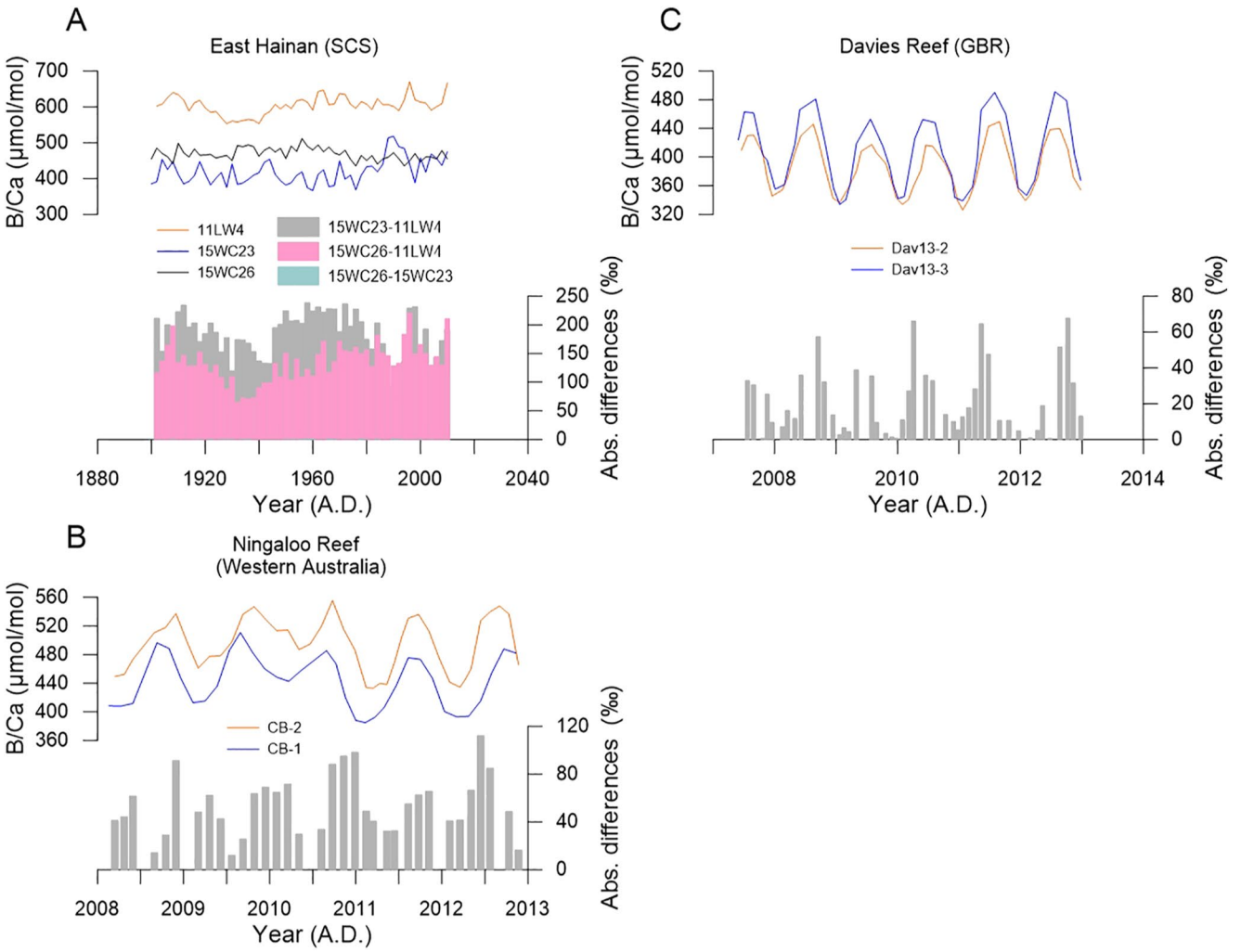

Figure 3. Assessment of B/Ca individual differences for *Porites* spp. corals. Comparisons between the coeval B/Ca determinations of corals from: (a) East Hainan Island (northern SCS, 11LW4 of Wei et al., 2015, 15WC23 and 15WC26 of this study); (b) Ningaloo Reef (Western Australia, M. T. McCulloch et al., 2017); and (c) Davies Reef (mid-shelf GBR, M. T. McCulloch et al., 2017), respectively. Absolute value of the difference between colonies is shown below each comparison. Note that B/Ca records in (a) are biennially resolved, while in panels (c and d) are monthly-resolved.

and 15WC26 (Figure 3a, Table 2), respectively, much above the 2σ of the magnitude of analytical precision (57.2 μmol/mol). However, smaller avg_{abs} was found between the adjacent two corals 15WC23 and 15WC26 (56.7 μmol/mol), and between the monthly B/Ca records (21.0 μmol/mol for Davies Reef and 59.9 μmol/mol for Ningaloo Reef; McCulloch et al., 2017; Figures 3b and 3c, Table 2). Generally, the mean offset of B/Ca between colonies showed an equivalent level with the respective avg_{abs} (Table 2), all pointing to considerable intercolony differences in skeletal B/Ca values. When combined with $\delta^{11}B$-pH_{cf} to convert B/Ca into the DIC_{cf}, it showed a much greater individual difference in coral DIC_{cf}, with mean difference up to 1,444 μmol/kg (Table 2).

3.2. Skeletal Boron Systematics and the Estimation of Coral CF Carbonate Chemistry in the Northern SCS Over the Past Millennium

The $\delta^{11}B$ values of the three modern corals from Hainan Is. varied from 21.5 to 25.5‰, exhibiting no significant long-term decline trend for the past 110 years (1900–2010; Figure 4). Despite showing significant individual differences as mentioned above, the cores had an average $\delta^{11}B$ level of 23.92 ± 0.82‰ (SD), which was comparable to the records derived from the south coast of Hainan Island and also fell within the global $\delta^{11}B$ range for *Porites* spp. corals (Figure 5). To better extract environmental signals, composite records were

Table 2
B/Ca Individual Differences of Porites spp. Corals

Sample resolution	Location	Sample name	B/Ca variation range	Analytical precision (2σ)	Mean value		Mean difference		Average absolute difference	
					B/Ca	DIC_{cf}	B/Ca	DIC_{cf}	B/Ca (SD)	DIC_{cf} (SD)
Biennial	Hainan Island South China Sea	11LW4	552.8–669.8	28.60	602.9	3,396	183.1[a]	1444[a]	183.7 (39.2) [a]	1,443 (425) [a]
		15WC23	366.5–517.9		419.8	4,840	48.8[b]	580[b]	56.7 (33.0) [b]	664 (230) [b]
		15WC26	435.0–511.7		468.6	4,260	134.3[c]	864[c]	135.3 (33.3) [c]	866 (416) [c]
Monthly	Davies Reef Mid-shelf GBR	Dav13-2[d]	326.1–449.3	NA	384.0	5,549	22.3	277	21 (17.8)	257 (210)
		Dav13-3[d]	333.7–491.2		406.3	5,272				
	Ningaloo Reef	CB-1[d]	385.0–522.9		442.4	4,868	59.0	547	59.9 (24.7)	625 (419)
		CB-2[d]	434.2–527.7		501.4	4,321				

[a]Difference was calculated from 15WC23-11LW4. [b]Difference was calculated from 15WC26-15WC23. [c]Difference was calculated from 15WC26-11LW4. [d]Data from M. T. McCulloch et al. (2017).

obtained for the common period 1900–2010. The data of each core were first normalized to the respective mean value according to the equation: $n_t = x_t - \overline{x_c}$, where x_t is the $\delta^{11}B$ value at a certain year and $\overline{x_c}$ is the mean $\delta^{11}B$ value for a given coral. Then, we took the average of the normalized data ($\overline{n_t}$) at a certain year and added with the average mean value of all three cores ($\overline{x_{all}}$) to preserve the units, i.e., $N_t = \overline{n_t} + \overline{x_{all}}$. The final results (Figure 4) showed a marginal long-term decline trend superimposed on the inter-decadal variations, with this decline being more prominent for the period of 1900–1978 (linear regression, df = 44, $p < 0.05$).

In contrast, the fossil corals showed higher $\delta^{11}B$, with values varying from 23.5 to 27.5‰ (Figure 4) and averaging at 25.59 ± 0.52‰ (SD, Figure 5). The mean $\delta^{11}B$ value of each fossil coral is consistently higher (by 1.25–2.32‰) than that of the modern corals, with a mean difference of ~1.67‰ between them. Two-sample *t* test (Table S4 in Supporting Information S1) also suggested that the $\delta^{11}B$ values for the two groups of corals were significantly different ($p < 0.01$). Differences also existed within the four fossils, with the mean difference between each other varying from 0.48 to 1.07‰. According to coral's U-Th ages and the noted climate anomalies for the last millennium, we grouped them into the LIA corals (13OC4 and 11LW2) and the MCA corals (11QG1 and 11QG3). Within each group, mean $\delta^{11}B$ difference was relatively small (0.01‰ and 0.48‰), below the 2σ of the magnitude of analytical precision (0.80‰), while the mean difference between the LIA and MCA was slightly higher with value of 0.82‰.

Skeletal B/Ca ratios of each coral record also exhibited inter-annual to decadal variations (Figure 4), and varied more dramatically among the three modern corals compared to the fossil (Figure 5). Mean difference for the coeval B/Ca determinations of the modern corals was as high as 183.7 μmol/mol, while the B/Ca records of fossil corals showed relatively smaller differences, with an average of 42.8 μmol/mol. The mean offset between the MCA and the LIA corals or between the fossil and modern corals is also small, with the value of 51.9 μmol/mol and of 51.3 μmol/mol, respectively, all below the 2σ of the magnitude of analytical precision (57.2 μmol/mol). Including the previously reported B/Ca results (mainly from the Australia corals), all modern corals had a mean level of 493.5 ± 78.6 μmol/mol (SD, Figure 5), showing no significant difference ($t = -1.92$, df = 11, $p = 0.08$; two-sample *t* test) in comparison with the fossil corals from the Hainan Island which averaged at 537.3 ± 38.1 μmol/mol (SD, Figure 5), in consideration of analytical precision or intercolony differences. Nevertheless, it appears that B/Ca values of all the fossil corals fell in the upper region of the modern range. Composite records of B/Ca were also calculated following the same manner aforementioned, exhibiting a long-term increasing trend (linear regression, df = 51; $p < 0.05$) for the recent 110 years.

Converting boron systematics into the carbonate chemistry of coral CF suggested a typically higher pH_{cf} of 8.59 for the fossil corals, significantly different from the modern corals (8.47, Table 3), with *p*-value below 0.05 (two-sample *t* test; Table S4 in Supporting Information S1), but no distinct changes in coral DIC_{cf} levels (3,621 μmol/kg for the fossil corals and 4,166 μmol/kg for the modern corals; $p > 0.05$; two-sample *t* test; Table S4 in Supporting Information S1) throughout the past millennium (Figure 4). Furthermore, although

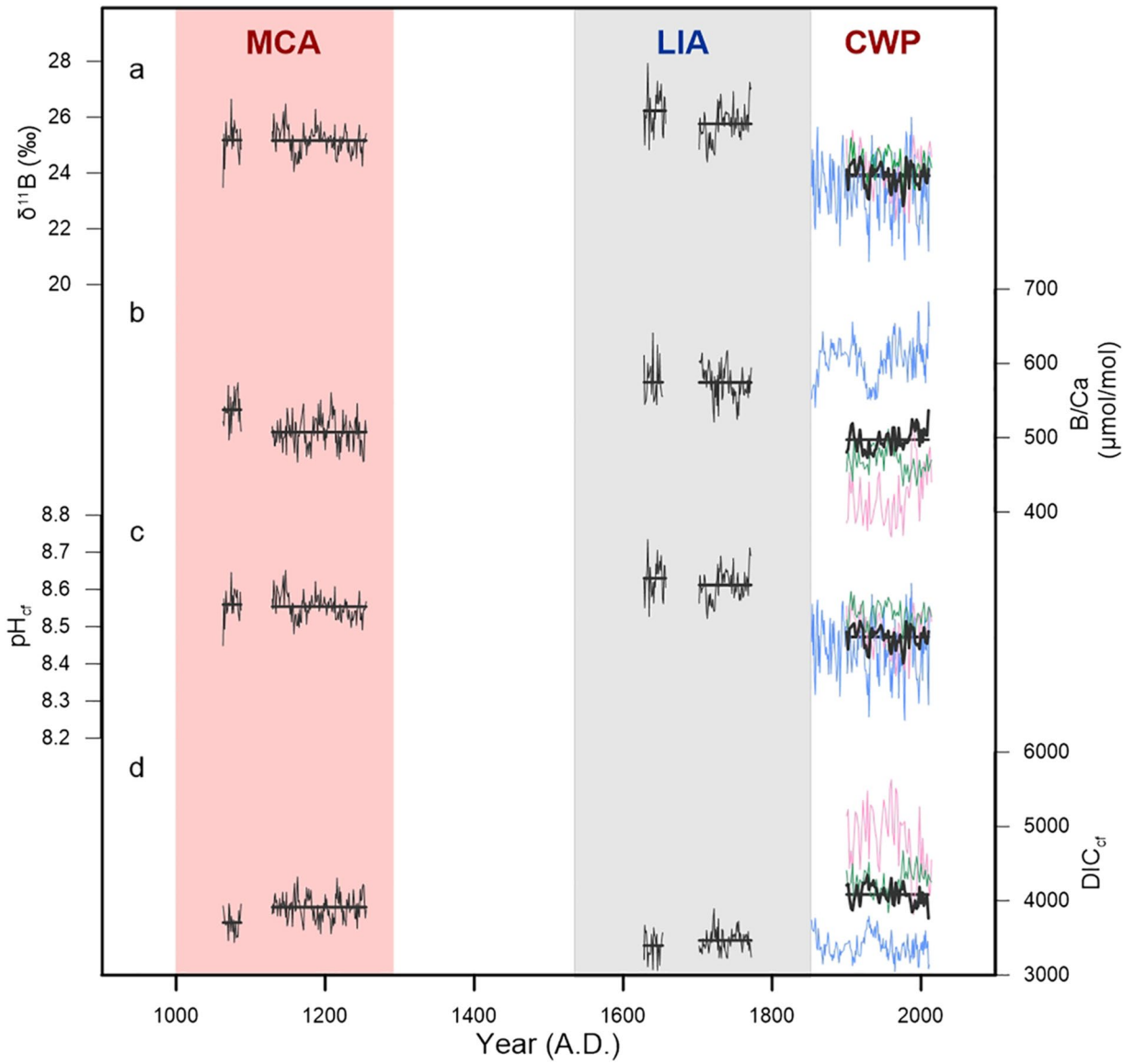

Figure 4. Boron systematics of the modern and fossil *Porites* spp. corals from the east Hainan Is. and the estimates for the carbonate chemistry of coral calcifying fluid: (a) $\delta^{11}B$, (b) B/Ca, (c) pH_{cf}, and (d) DIC_{cf}. Data for the modern corals are colored with blue for 11LW4, pink for 15WC23, and green for 15WC26, and bold black for the composite records. Mean average for each record is also indicated with the straight line.

it also seemed that the LIA corals tended to have a higher pH_{cf} compared to the MCA, the offset between the two groups of corals was only about 0.07, comparable to the mean offset of coral pH_{cf} (0.07) and below the estimated largest intercolony differences in pH_{cf} (0.08, Table 1). More samples need to be included to ascertain this difference. The negative relationship between coral pH_{cf} and DIC_{cf}, commonly observed in the previously reported corals (e.g., Chen et al., 2019; D'Olivo et al., 2017, 2019; McCulloch et al., 2017), remains significant in the Hainan corals, with the exception of 11LW4 (Table 3). It is unclear why no significant correlation of pH_{cf}-DIC_{cf} is found for 11LW4, but we speculate that the heterogeneity of coral CF chemistry (Chalk et al., 2021) or the sampling positions (Reed et al., 2021) may result in the lack of correlation between the measurements of B/Ca and $\delta^{11}B$ from two different sets of powder samples.

The pH_{sw}, estimated from $\delta^{11}B$-derived pH_{cf}, exhibited an evident offset (~0.24 pH units) between the pre- and post-industrial periods with average values of 8.29 and 8.05, respectively (Table 3). This suggests a prominent seawater pH decline in the east coast of Hainan Island.

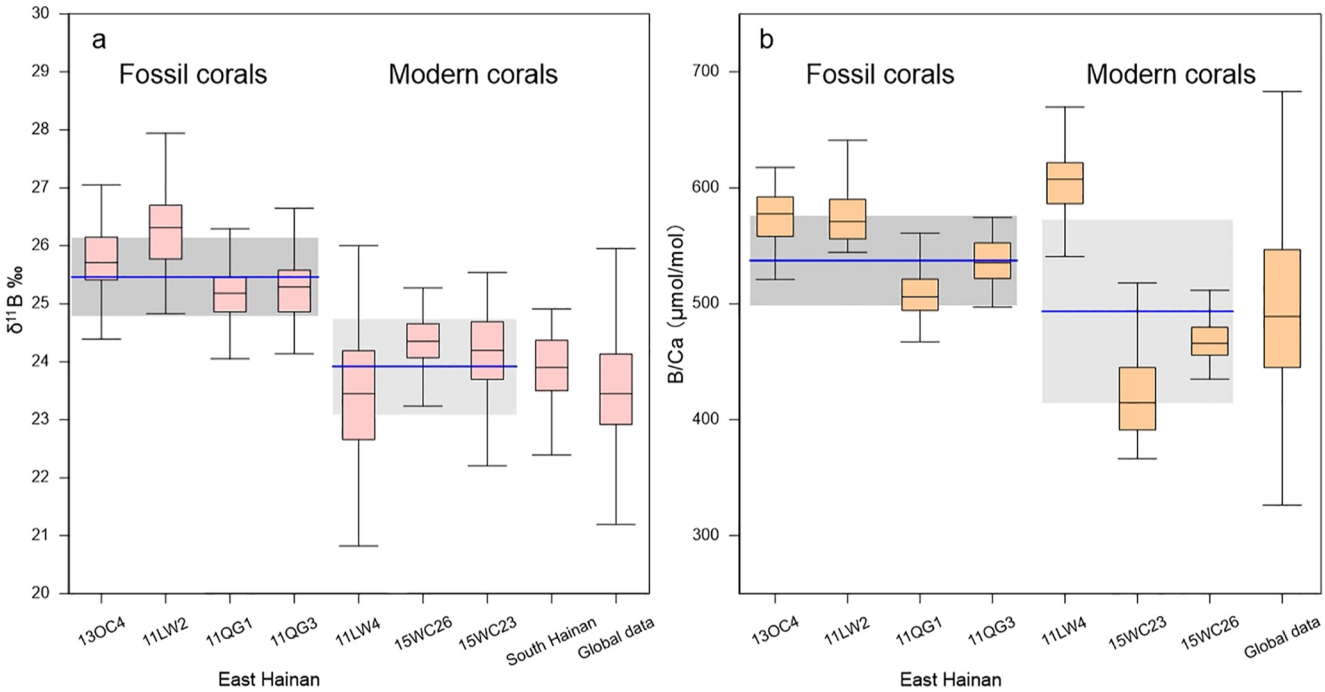

Figure 5. Box-whisker plots of skeletal $\delta^{11}B$ and B/Ca in the modern and fossil corals from the Hainan Is. in the northern South China Sea. For comparison, global data sets of boron systematics for the *Porites* spp. are also shown, including Chen et al. (2019), D'Olivo et al. (2015, 2019), Kubota et al. (2017), M. T. McCulloch et al. (2017), Pelejero et al. (2005), Shinjo et al. (2013) and Wei et al. (2009, 2015). The blue lines indicate the mean average with the standard deviation shown as the shaded area.

4. Discussion

4.1. Intercolony Differences in Coral Boron Systematics

Replication tests show that corals from the same reef environment can exhibit considerable absolute differences (or mean differences) in their coeval boron systematics (Figures 2 and 3), with this divergence being much larger for annually-biennially resolved records. Two-sample *t* tests (Table S2 in Supporting Information S1) indicate that, with the exception of corals from the Ningaloo Reef and the two adjacent colonies from the Hainan Island (15WC23 and 15WC26), the other sets of corals show significant differences ($p < 0.05$) in their coeval $\delta^{11}B$ determinations. Moreover, even with analytical precision being accounted for, only 3 out of 9 $\delta^{11}B$ comparisons show acceptable avg_{abs} values ($<2\sigma$ the magnitude of analytical precision). As for B/Ca, the three sets of corals all exhibit significant differences ($p < 0.05$, two-sample *t* tests, Table S3 in Supporting Information S1), and 2 out of 5 comparisons show avg_{abs} or mean difference below the 2σ the magnitude of analytical precision. Accordingly, these all point to considerable intercolony differences in coral boron systematics, with the mean offset as high as 1.05‰ for $\delta^{11}B$ and 183.1 μmol/mol for B/Ca. Additionally, the variation pattern of annual-biennial records are also not consistent within each set of corals, barely showing any correlation between each other, even for the colonies growing within 5 m distance (15WC23 and 15WC26, 10AR2 and AREO 4). Although certain studies (Wei et al., 2015; Wu et al., 2018) have demonstrated a good replication of $\delta^{11}B$ record within the same colony, our study suggests a poor $\delta^{11}B$ (as well as B/Ca) replication among different colonies, in particular for the annual- and biennial-resolution records.

Table 3
Boron Systematics and Estimated Carbonate Chemistry in Coral Calcifying Fluid

Sample name	Climate epoch	$\delta^{11}B$	pH_{cf}	pH_{sw}	B/Ca	DIC	pH_{cf}-DIC_{cf} [a]
Modern corals							
11LW4	CWP	23.34	8.43	8.00	604.2	3,396	-
15WC23		24.10	8.48	8.06	419.8	4,840	−0.70
15WC26		24.31	8.50	8.09	468.6	4,260	−0.60
Average		23.92	8.47	8.05	497.5	4,166	/
Fossil corals							
13OC4	LIA	25.76	8.63	8.38	574.5	3,468	−0.44
11LW2		26.24	8.61	8.34	574.7	3,398	−0.70
11QG1	MCA	25.17	8.55	8.21	507.6	3,913	−0.45
11QG3		25.18	8.56	8.22	537.8	3,706	−0.38
Average		25.59	8.59	8.29	548.6	3,621	/

[a]Correlation with $p > 0.05$.

This intercolony difference in coral boron systematics is likely a manifestation of large inherent difference in coral CF carbonate chemistry, with the average of absolute difference as high as 0.08 for pH_{cf} and 1,444 μmol/kg for DIC_{cf}. Since our intercolony differences evaluation includes colonies from different sites within the same reef, it is possibly that micro-environmental pH or DIC effects might also contribute to such difference, as seawater provides the basic supply for coral CF. However, for corals growing next to each other with minimal micro-environmental effects, we still find moderate absolute difference between them. This hints that the physiological differences of corals offer each colony a different capability to control its internal CO_2 system and to up-regulate the internal pH_{cf}, resulting in great intercolony differences in CF carbonate chemistry. Furthermore, since these *Porites* corals are not identified at a species level, interspecific differences may also contribute to some of this observed intercolony differences.

4.2. Variation in CF Carbonate Chemistry Over the Past Millennium

Coral pH_{cf} appears to exhibit a marginal increase from the MCA to LIA, followed by a considerable decrease to the Current Warm Period (CWP, standing for the post-industrial warming period; Figure 4). However, taking the intercolony differences into consideration, the pH_{cf} offset between the MCA and LIA corals is ~0.07, slightly below the upper limit of the observed pH_{cf} individual differences (0.08; Table 1), comparable to the mean offset of coeval coral pH_{cf} (0.07; Table 1). Thus, the conclusion that there is a shift toward higher pH_{cf} for the LIA corals remains uncertain until more fossil corals are included. Taking all fossil corals as a whole, the pre-industrial pH_{cf} level (8.59, estimated from 4 colonies) is ~0.12 higher than that of the post-industrial level (8.47, estimated from 3 colonies). The value exceeds the estimated individual pH_{cf} difference (0.08, Table 1), suggesting considerable pH_{cf} decline for the modern corals in this region. Another modern coral (Song-5, Figure 1) from the south coast of Hainan Island also exhibits a similar lower pH_{cf} level compared to the fossil corals with a mean value of 8.49 (1841–2001; Liu et al., 2014), corroborating the reduced coral pH_{cf} in the nearshore Hainan Island and suggesting significantly negative impact of OA on coral pH_{cf}.

By contrast, despite of evident declines in coral pH_{cf}, it appears that the DIC_{cf} of *Porites*, even when only the post-1980 data (during which warming begins to suppress coral symbiosis and metabolism) are considered, shows no significant changes throughout the past 1 ka. This suggests that corals' ability to concentrate carbon for calcification have not been significantly disturbed by anthropogenic impacts, such as ocean warming or nearshore activities in this region. However, it should be noted that our data sets involve a small number of coral samples, and thereof there is possibility that the striking intercolony differences of DIC_{cf} might obscure any changes in DIC_{cf} induced by anthropogenic forcing.

4.3. Implications for Seawater pH Changes

The reconstructed pH_{sw} from each fossil coral record shows comparable average levels within the respective climate epoch, with mean values of 8.22 and 8.36 for the MCA and LIA, respectively. This yields a difference of approximately 0.14 units for coral-derived pH_{sw} between the MCA and LIA, which is, however, equals to the largest pH reconstruction bias estimated from the coral $\delta^{11}B$ intercolony differences. More coral samples are needed to confirm this pH_{sw} changes between the two notable climate epochs over the last millennium. Nevertheless, the estimated mean pH_{sw} value (~8.29) from all fossil corals ($n = 4$) is much higher than that of the modern record (~8.05; $n = 3$), indicating a more marked pH_{sw} decrease of ~0.24 from the LIA to the CWP. This prominent pH_{sw} decline exceeds the modeled global average pH_{sw} reduction induced by OA (~0.10, Orr et al., 2005), but is comparable to the OA estimation in the nearshore south Hainan (~0.24, Liu et al., 2014) and in the California Current Ecosystem (~0.21, Osborne et al., 2020).

The striking pH_{sw} decline, occurring around the transition from the LIA to CWP, leads us to speculate that increased atmospheric CO_2 from the mid-19th century may contribute greatly to this reduction (Figure 6), since the uptake of CO_2 by the ocean is one of the major factors driving pH_{sw} changes, especially modern OA (Feely et al., 2004). Therefore, we plot our coral records with another pH_{sw} reconstruction from the south Hainan Is. (Liu et al., 2014) as well as the atmospheric CO_2 concentration (Figure 6). It appears that the overall coral pH_{sw} reconstruction follows the atmospheric CO_2 changes, with higher pH_{sw} levels and no significant centennial variability during the pre-industrial era, but lower pH_{sw} levels and a long-term decline for the industrial era (Figure 6). However, the composite pH_{sw} reconstruction derived from the modern

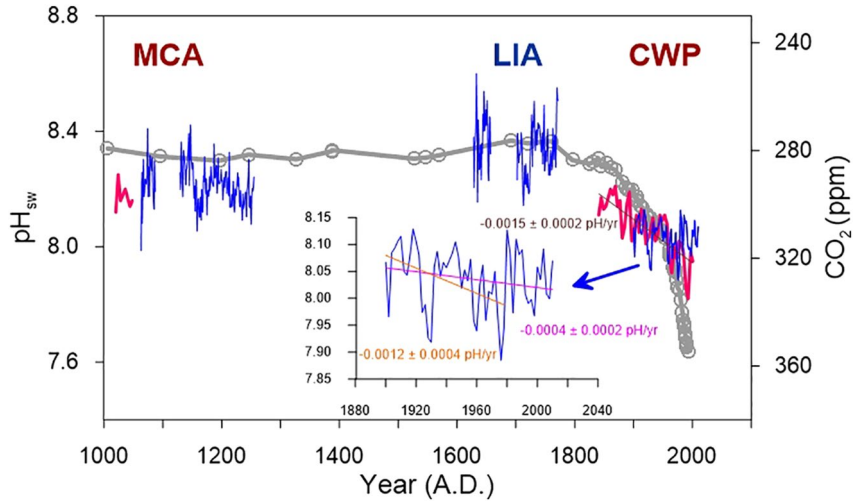

Figure 6. Comparison between atmospheric CO_2 concentration and coral-derived pH_{sw} reconstructions in the nearshore Hainan Island of the northern SCS over the past millennium. Records for the east coast are shown with blue lines, with a close-up of modern composite records shown in the inset. Records of the south coast (Liu et al., 2014) are shown with red lines. Despite exhibiting a marginal declines (of −0.0004 ± 0.0002 pH/year) for the period of 1900–2010, pH_{sw} of the east coast reduced more prominently (−0.0012 ± 0.0004 pH/year) from 1900 to 1978 with this decline rate comparable to the estimation for the south coast −0.0015 ± 0.0002 pH/year; 1847–2001). Note that atmospheric CO_2 concentration is plotted on an inverted scale on the *y* axis, with data from Keeling et al. (2001).

corals (CE 1900–2010, $n = 3$; Figure 6) exhibits an overall slow decline rate of −0.0004 ± 0.0002 pH/years, which could only result in about 0.04 ± 0.02 pH_{sw} decline for the past 110 years. This slow decline rate is likely a result of elevated pH_{sw} level from 1980 onwards (Figure 6), because we find a more prominent pH_{sw} decline with a rate of −0.0012 ± 0.0004 pH/year for the period of 1900–1978, which is basically comparable to the rapid decline rate of −0.0015 ± 0.0002 pH/year (CE 1841–2001) in the south coast of Hainan Island (Liu et al., 2014). This suggests that east Hainan Island has also experienced significant ocean acidification over the past century. However, it seems that other local processes have come into play in recent 30 year, which likely have alleviated the CO_2-induced OA effect in this region, as the pace of pH_{sw} decline slows. This highlights the importance of a further understanding of the pH_{sw} regulation by local physical or biological processes and their interactions with OA, to offer a better projection for the future situation.

5. Conclusions

Coral $\delta^{11}B$ and B/Ca exhibit considerable intercolony differences, with mean offset as large as 1.05‰ and 183.1 μmol/mol, respectively. This indicates that splicing coral boron systematic records to generate long-term reconstruction of coral CF chemistry and pH_{sw} variation carries great risks, in particular without coeval replication records.

Our estimation from $\delta^{11}B$ and B/Ca records of 4 fossil and 3 modern corals in the northern SCS suggest that, the pH_{cf} of modern corals has shifted to lower values compared to the fossil with an average decline of 0.12, but the DIC_{cf} changes is less noticeable though the B/Ca ratios of fossil corals all fall in the upper region of the modern range. The pH_{cf} decline, likely an effect of ocean acidification, highlights significant anthropogenic influences on corals' capacity to up-regulate pH at their calcification site, which is central to coral resilience to OA, thereof making corals more vulnerable to future climate change.

The overall coral pH_{sw} reconstruction over the past millennium seems to follow the variation of atmospheric CO_2 concentration, demonstrating significant CO_2-induced ocean acidification in the northern SCS. Nevertheless, in the east coast of Hainan Island, pH_{sw} has staged a recovery since the 1980, slowing down the OA rate, hinting a compensating effect from local physical or biological processes, and underlining the important roles of local natural forcing in regulating pH_{sw}.

Data Availability Statement

Data set for this article can be found at Chen et al. (2021): $\delta^{11}B$ and B/Ca measurements of the modern and fossil *Porites* corals from the east coast Hainan Island in the northern South China Sea. Zenodo (https://doi.org/10.5281/zenodo.4896184).

Acknowledgments
This work was financially supported by the Strategic Priority Research Program of Chinese Academy of Sciences (Grant No. XDB40010300), the National Key Research and Development Project of China (2016YFA0601204), and the Key Special Project for Introduced Talents Team of Southern Marine Science and Engineering Guangdong Laboratory (Guangzhou) (GML2019ZD0308). X.C. thanks the funding support from the National Natural Science Foundation of China (41803017), Guangdong Basic and Applied Basic Research Foundation (2019A1515010892), the Youth Innovation Promotion Association of the Chinese Academy of Sciences (2021352) and the Tuguangchi Award for Excellent Young Scholar from the GIG-CAS. This is contribution No. IS-3079 from the GIG-CAS.

References

Chalk, T. B., Standish, C. D., D'Angelo, C., Castillo, K. D., Milton, J. A., & Foster, G. L. (2021). Mapping coral calcification strategies from in situ boron isotope and trace element measurements of the tropical coral *Siderastrea siderea*. *Scientific Reports*, *11*(1), 472. https://doi.org/10.1038/s41598-020-78778-1

Chen, X., D'Olivo, J. P., Wei, G., & McCulloch, M. (2019). Anthropogenic ocean warming and acidification recorded by Sr/Ca, Li/Mg, $\delta^{11}B$, and B/Ca in Porites coral from the Kimberley region of northwestern Australia. *Palaeogeography, Palaeoclimatology, Palaeoecology*, *528*, 50–59. https://doi.org/10.1016/j.palaeo.2019.04.033

Chen, X., Wei, G., Deng, W., Liu, Y., Sun, Y., Zeng, T., & Xie, L. (2015). Decadal variations in trace metal concentrations on a coral reef: Evidence from a 159 yr record of Mn, Cu, and V in a Porites coral from the northern South China Sea. *Journal of Geophysical Research: Oceans*, *120*(1), 405–416. https://doi.org/10.1002/2014jc010390

Cobb, K. M., Charles, C. D., Cheng, H., & Edwards, R. L. (2003). El Nino/Southern Oscillation and tropical Pacific climate during the last millennium. *Nature*, *424*(6946), 271–276. https://doi.org/10.1038/nature01779

D'Olivo, J. P., Ellwood, G., DeCarlo, T. M., & McCulloch, M. T. (2019). Deconvolving the long-term impacts of ocean acidification and warming on coral biomineralization. *Earth and Planetary Science Letters*, *526*, 115785. https://doi.org/10.1016/j.epsl.2019.115785

D'Olivo, J. P., & McCulloch, M. T. (2017). Response of coral calcification and calcifying fluid composition to thermally induced bleaching stress. *Scientific Reports*, *7*(1), 2207. https://doi.org/10.1038/s41598-017-02306-x

D'Olivo, J. P., McCulloch, M. T., Eggins, S. M., & Trotter, J. (2015). Coral records of reef-water pH across the central Great Barrier Reef, Australia: Assessing the influence of river runoff on inshore reefs. *Biogeosciences*, *12*(4), 1223–1236. https://doi.org/10.5194/bg-12-1223-2015

Deng, W., Chen, X., Wei, G., Zeng, T., & Zhao, J.-X. (2017). Decoupling of coral skeletal $\delta^{13}C$ and solar irradiance over the past millennium caused by the oceanic Suess effect. *Paleoceanography*, *32*(2), 161–171. https://doi.org/10.1002/2016pa003049

Deng, W., Liu, X., Chen, X., Wei, G., Zeng, T., Xie, L., & Zhao, J.-X. (2017). A comparison of the climates of the Medieval Climate Anomaly, Little Ice Age, and Current Warm Period reconstructed using coral records from the northern South China Sea. *Journal of Geophysical Research: Oceans*, *122*(1), 264–275. https://doi.org/10.1002/2016jc012458

Deng, W., Wei, G., Xie, L., Ke, T., Wang, Z., Zeng, T., & Liu, Y. (2013). Variations in the Pacific Decadal Oscillation since 1853 in a coral record from the northern South China Sea. *Journal of Geophysical Research: Oceans*, *118*(5), 2358–2366. https://doi.org/10.1002/jgrc.20180

Dickson, A. G. (1990). Thermodynamics of the dissociation of boric-acid in synthetic seawater from 273.15 to 318.15 K. *Deep Sea Research Part A. Oceanographic Research Papers*, *37*(5), 755–766. Doi https://doi.org/10.1016/0198-0149(90)90004-F

Dong, X., Huang, H., Zheng, N., Pan, A., Wang, S., Huo, C., et al. (2017). Acidification mediated by a river plume and coastal upwelling on a fringing reef at the east coast of Hainan Island, Northern South China Sea. *Journal of Geophysical Research-Oceans*, *122*(9), 7521–7536. https://doi.org/10.1002/2017jc013228

Douville, E., Paterne, M., Cabioch, G., Louvat, P., Gaillardet, J., Juillet-Leclerc, A., & Ayliffe, L. (2010). Abrupt sea surface pH change at the end of the Younger Dryas in the central sub-equatorial Pacific inferred from boron isotope abundance in corals (*Porites*). *Biogeosciences*, *7*(8), 2445–2459. https://doi.org/10.5194/bg-7-2445-2010

Feely, R. A., Sabine, C. L., Lee, K., Berelson, W., Kleypas, J., Fabry, V. J., & Millero, F. J. (2004). Impact of anthropogenic CO_2 on the $CaCO_3$ system in the oceans. *Science*, *305*(5682), 362–366. https://doi.org/10.1126/science.1097329

Foster, G. L., Pogge von Strandmann, P. A. E., & Rae, J. W. B. (2010). Boron and magnesium isotopic composition of seawater. *Geochemistry, Geophysics, Geosystems*, *11*(8), Q08015. https://doi.org/10.1029/2010gc003201

Fowell, S. E., Foster, G. L., Ries, J. B., Castillo, K. D., Vega, E., Tyrrell, T., et al. (2018). Historical trends in pH and carbonate biogeochemistry on the Belize Mesoamerican Barrier Reef System. *Geophysical Research Letters*, *45*(7), 3228–3237. https://doi.org/10.1002/2017gl076496

Gagan, M., Ayliffe, L., Beck, J., Cole, J., Druffel, E., Dunbar, R., & Schrag, D. (2000). New views of tropical paleoclimates from corals. *Quaternary Science Reviews*. *19*(1), 45–64. https://doi.org/10.1016/s0277-3791(99)00054-2

Goodkin, N. F., Wang, B. S., You, C. F., Hughen, K. A., Grumet-Prouty, N., Bates, N. R., & Doney, S. C. (2015). Ocean circulation and biogeochemistry moderate interannual and decadal surface water pH changes in the Sargasso Sea. *Geophysical Research Letters*, *42*(12), 4931–4939. https://doi.org/10.1002/2015gl064431

Hönisch, B., Hemming, N. G., Grottoli, A. G., Amat, A., Hanson, G. N., & Bijma, J. (2004). Assessing scleractinian corals as recorders for paleo-pH: Empirical calibration and vital effects. *Geochimica et Cosmochimica Acta*, *68*(18), 3675–3685. https://doi.org/10.1016/j.gca.2004.03.002

Hathorne, E. C., Gagnon, A., Felis, T., Adkins, J., Asami, R., Boer, W., et al. (2013). Interlaboratory study for coral Sr/Ca and other element/Ca ratio measurements. *Geochemistry, Geophysics, Geosystems*, *14*(9), 3730–3750. https://doi.org/10.1002/ggge.20230

Hemming, N. G., & Hanson, G. N. (1992). Boron isotopic composition and concentration in modern marine carbonates. *Geochimica et Cosmochimica Acta*, *56*(1), 537–543. https://doi.org/10.1016/0016-7037(92)90151-8

Hemming, N. G., Reeder, R. J., & Hart, S. R. (1998). Growth-step-selective incorporation of boron on the calcite surface. *Geochimica et Cosmochimica Acta*, *62*(17), 2915–2922. https://doi.org/10.1016/s0016-7037(98)00214-2

Hoegh-Guldberg, O., Mumby, P. J., Hooten, A. J., Steneck, R. S., Greenfield, P., Gomez, E., et al. (2007). Coral reefs under rapid climate change and ocean acidification. *Science*, *318*(5857), 1737–1742. https://doi.org/10.1126/science.1152509

Holcomb, M., DeCarlo, T. M., Gaetani, G. A., & McCulloch, M. (2016). Factors affecting B/Ca ratios in synthetic aragonite. *Chemical Geology*, *437*, 67–76. https://doi.org/10.1016/j.chemgeo.2016.05.007

Keeling, C. D., Piper, S. C., Bacastow, R. B., Wahlen, M., Whorf, T. P., Heimann, M., & Meijer, H. A. (2001). Exchanges of atmospheric CO_2 and $^{13}CO_2$2 with the terrestrial biosphere and oceans from 1978 to 2000. I. Global aspects. SIO Reference Series, No. 01–06 (p. 88). Scripps Institution of Oceanography.

Klochko, K., Cody, G. D., Tossell, J. A., Dera, P., & Kaufman, A. J. (2009). Re-evaluating boron speciation in biogenic calcite and aragonite using 11B MAS NMR. *Geochimica et Cosmochimica Acta*, *73*(7), 1890–1900. https://doi.org/10.1016/j.gca.2009.01.002

Krief, S., Hendy, E. J., Fine, M., Yam, R., Meibom, A., Foster, G. L., & Shemesh, A. (2010). Physiological and isotopic responses of scleractinian corals to ocean acidification. *Geochimica et Cosmochimica Acta*, *74*(17), 4988–5001. https://doi.org/10.1016/j.gca.2010.05.023

Kubota, K., Yokoyama, Y., Ishikawa, T., Suzuki, A., & Ishii, M. (2017). Rapid decline in pH of coral calcification fluid due to incorporation of anthropogenic CO_2. *Scientific Reports*, *7*(1), 7694. https://doi.org/10.1038/s41598-017-07680-0

Liu, Y., Liu, W., Peng, Z., Xiao, Y., Wei, G., Sun, W., et al. (2009). Instability of seawater pH in the South China Sea during the mid-late Holocene: Evidence from boron isotopic composition of corals. *Geochimica et Cosmochimica Acta*, *73*(5), 1264–1272. https://doi.org/10.1016/j.gca.2008.11.034

Liu, Y., Peng, Z. C., Zhou, R. J., Song, S. H., Liu, W. G., You, C. F., et al. (2014). Acceleration of modern acidification in the South China Sea driven by anthropogenic CO_2. *Scientific Reports*, *4*. https://doi.org/10.1038/srep05148

McCulloch, M., Falter, J., Trotter, J., & Montagna, P. (2012). Coral resilience to ocean acidification and global warming through pH up-regulation. *Nature Climate Change*, *2*(8), 623–627. https://doi.org/10.1038/nclimate1473

McCulloch, M. T., D'Olivo, J. P., Falter, J., Holcomb, M., & Trotter, J. A. (2017). Coral calcification in a changing world and the interactive dynamics of pH and DIC upregulation. *Nature Communications*, *8*, 15686. https://doi.org/10.1038/ncomms15686

McCulloch, M. T., Holcomb, M., Rankenburg, K., & Trotter, J. A. (2014). Rapid, high-precision measurements of boron isotopic compositions in marine carbonates. *Rapid Communications in Mass Spectrometry*, *28*(24), 2704–2712. https://doi.org/10.1002/rcm.7065

Orr, J. C., Fabry, V. J., Aumont, O., Bopp, L., Doney, S. C., Feely, R. A., et al. (2005). Anthropogenic ocean acidification over the twenty-first century and its impact on calcifying organisms. *Nature*, *437*(7059), 681–686. https://doi.org/10.1038/nature04095

Osborne, E. B., Thunell, R. C., Gruber, N., Feely, R. A., & Benitez-Nelson, C. R. (2020). Decadal variability in twentieth-century ocean acidification in the California Current Ecosystem. *Nature Geoscience*, *13*(1), 43–49. https://doi.org/10.1038/s41561-019-0499-z

Pelejero, C., Calvo, E., McCulloch, M. T., Marshall, J. F., Gagan, M. K., Lough, J. M., & Opdyke, B. N. (2005). Preindustrial to modern interdecadal variability in coral reef pH. *Science*, *309*(5744), 2204–2207. https://doi.org/10.1126/science.1113692

Raddatz, J., Liebetrau, V., Trotter, J., Rüggeberg, A., Flögel, S., Dullo, W.-C., et al. (2016). Environmental constraints on Holocene cold-water coral reef growth off Norway: Insights from a multiproxy approach. *Paleoceanography*, *31*(10), 1350–1367. https://doi.org/10.1002/2016pa002974

Reed, E. V., Thompson, D. M., Cole, J. E., Lough, J. M., Cantin, N. E., Cheung, A. H., et al. (2021). Impacts of coral growth on geochemistry: Lessons from the Galápagos Islands. *Paleoceanography and Paleoclimatology*, *36*(4), e2020PA004051. https://doi.org/10.1029/2020PA004051

Ross, C. L., Falter, J. L., & McCulloch, M. T. (2017). Active modulation of the calcifying fluid carbonate chemistry (δ^{11}B, B/Ca) and seasonally invariant coral calcification at sub-tropical limits. *Scientific Reports*, *7*(1), 13830. https://doi.org/10.1038/s41598-017-14066-9

Shinjo, R., Asami, R., Huang, K.-F., You, C.-F., & Iryu, Y. (2013). Ocean acidification trend in the tropical North Pacific since the mid-20th century reconstructed from a coral archive. *Marine Geology*, *342*, 58–64. https://doi.org/10.1016/j.margeo.2013.06.002

Tambutté, S., Holcomb, M., Ferrier-Pagès, C., Reynaud, S., Tambutté, É., Zoccola, D., & Allemand, D. (2011). Coral biomineralization: From the gene to the environment. *Journal of Experimental Marine Biology and Ecology*, *408*(1–2), 58–78. https://doi.org/10.1016/j.jembe.2011.07.026

Wei, G., McCulloch, M. T., Mortimer, G., Deng, W. F., & Xie, L. H. (2009). Evidence for ocean acidification in the Great Barrier Reef of Australia. *Geochimica et Cosmochimica Acta*, *73*(8), 2332–2346. https://doi.org/10.1016/j.gca.2009.02.009

Wei, G., Wang, Z., Ke, T., Liu, Y., Deng, W., Chen, X., et al. (2015). Decadal variability in seawater pH in the West Pacific: Evidence from coral δ^{11}B records. *Journal of Geophysical Research: Oceans*, *120*(11), 7166–7181. https://doi.org/10.1002/2015jc011066

Wu, H. C., Dissard, D., Douville, E., Blamart, D., Bordier, L., Tribollet, A., et al. (2018). Surface ocean pH variations since 1689 CE and recent ocean acidification in the tropical South Pacific. *Nature Communications*, *9*(1), 2543. https://doi.org/10.1038/s41467-018-04922-1

Zeebe, R. E., & Wolf-Gladrow, D. A. (2001). *CO_2 in seawater: Equilibrium, kinetics, isotopes*, Elsevier Science Limited.

References From the Supporting Information

Cheng, H., Edwards, R. L., Hoff, J., Gallup, C. D., Richards, D. A., & Asmerom, Y. (2000). The half-lives of uranium-234 and thorium-230. *Chemical Geology*, *169*(1–2), 17–33. https://doi.org/10.1016/s0009-2541(99)00157-6

Ludwig, K. R. (2003). *Users Manual for Isoplot/Ex version 3.0: A Geochronological Toolkit for Microsoft Excel*. Berkeley Geochronology Centre Special Publication No 3.